nature geoscience
SUPPLEMENTARY INFORMATION
DOI: 10.1038/NGEO941

The Oldest Pb-Pb Age of a Meteoritic Inclusion Redefines the Age of the Solar System

by A. Bouvier and M. Wadhwa

Materials and Methods

1) Petrographic description of the calcium aluminum-rich inclusion from NWA 2364

The calcium aluminum-rich inclusion (CAI) named 2364-B1 (Fig. S1) from the CV3 chondrite NWA 2364[1] studied here is a large (~1 cm across) spherical inclusion. A polished thick section was prepared from 3 small fragments (each ~2 mm across) from the interior of this inclusion (see following section on "Sample preparation") and was documented with the JEOL 845 scanning electron microscope (SEM) at Arizona State University (ASU).

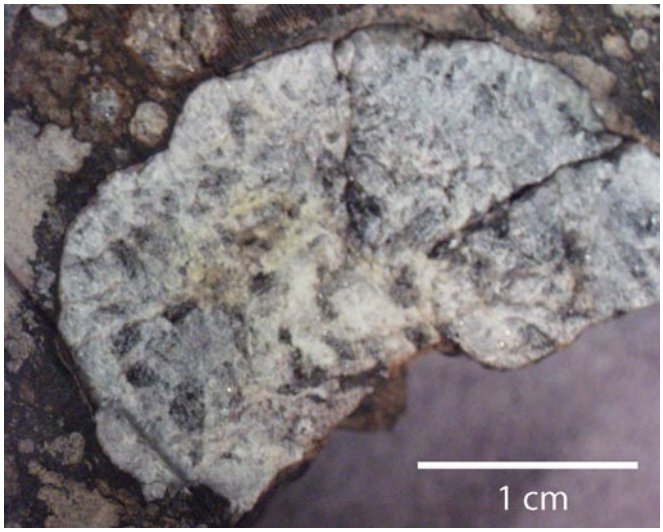

Fig. S1: A reflected light image (taken with a stereo microscope) of the CAI 2364-B1 from the NWA 2364 CV3 chondrite prior to being extracted from the meteorite slab.

DOI: 10.1038/NGEO941

The SEM investigation of this CAI (Fig. S2) revealed that this is an igneous-textured inclusion that contains coarse melilite (me; $(Ca,Na)_2(Al,Mg,Fe^{++})(Si,Al)_2O_7$), anorthite (an; $CaAl_2Si_2O_8$), spinel (sp; $MgAl_2O_4$), and fassaite (fa, Ti-rich augitic pyroxene; $Ca(Mg,Fe^{3+},Al)(Si,Al)_2O_6$). This inclusion was thus classified as a type-B CAI.

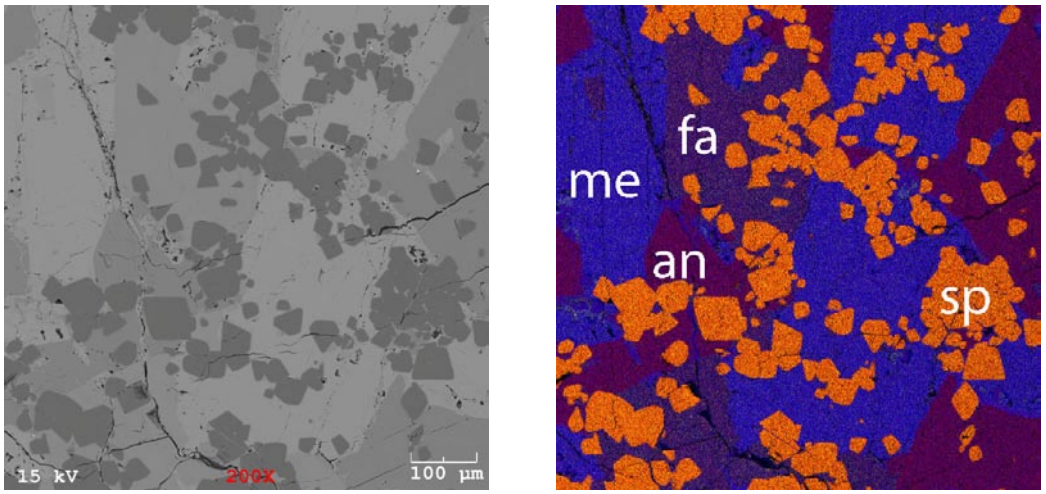

Fig. S2: Back-scattered electron image (left) and corresponding combined X-ray elemental maps (right) of Mg (yellow), Al (red), and Ca (blue) of the interior of NWA 2364 CAI obtained using the JEOL 845 SEM at ASU. me = melilite; fa = fassaite, an = anorthite, sp = spinel.

2) Sample preparation and chemical processing

All sample handling and processing was performed under clean laboratory conditions in the Isotope Cosmochemistry and Geochronology Laboratory (ICGL) at ASU. A ~500 mg piece of the type-B CAI 2364-B1 was extracted from a slab (4 × 3 × 0.7 mm) of the NWA 2364 CV3 chondrite using pre-cleaned tungsten tools. This piece was ultrasonicated for 5 minutes and rinsed in Milli-Q H_2O, and thereafter coarsely crushed in an agate mortar (which was pre-cleaned in 15% HNO_3 and Milli-Q water successively, for ~12 hours each). Fragments of the inclusion were then carefully hand-selected to avoid pieces that contained any attached matrix.

Fragments from the interior and rim portions of 2364-B1 CAI were then separated by hand, and were processed separately. Three small interior fragments (each ~2 mm across) were mounted into a polished section for petrographic documentation, while the remaining fragments were processed for ^{207}Pb-^{206}Pb and ^{26}Al-^{26}Mg isotopic analyses.

Sample preparation and chemical procedures for Pb-Pb analyses:

For the Pb-Pb analyses, two bulk fractions, one composed of interior fragments and another of rim fragments, were hand picked. Additionally, another fraction consisting of interior fragments was crushed in the agate mortar and then sieved. From the 63-100 μm size fraction of this sieved interior sample, metal was first separated using a hand-magnet, and then density separates were obtained using methylene iodide (Geoliquids®, d=3.30-3.33). The density separated samples were thoroughly rinsed with acetone, and then handpicked to obtain melilite-anorthite-rich and fassaite-rich fractions. A small portion of each of the three interior fractions was reserved for Al-Mg analyses (see section below on "Sample preparation and chemical procedures for Al-Mg analyses"). Subsequently, we acid-leached the following four samples of the 2364-B1 CAI that were prepared as described above: a bulk fraction from the interior (#1), two mineral separates (#2, fassaite-rich and #3, melilite-anorthite-rich) from the interior, and a bulk fraction composed of the rim (#4). The acid-leaching protocol used by us is similar to the protocol used by Connelly et al.[2] and included 7 steps (with the respective leachates denoted as L_1, L_2,…L_7) using different types and concentrations of acids at room temperature and ultrasonication for 15 to 30 minutes (except when noted otherwise) in the following order: 1.5M HBr (15 min), 1M HNO_3 (20 min), 2.5M HCl (30 min), 6M HCl (30 min), 6M HCl (100°C, 6 hr, and 15 min ultrasonication), 1M HF (30 min), and 1M HF (100°C, 12 hr, and 15 min

DOI: 10.1038/NGEO941

ultrasonication). Leachates were dried down and, along with the residues (denoted as R), fully dissolved in concentrated HF:HNO_3 (5:1) at 130°C in PFA Savillex® beakers, and converted to the chloride form before Pb extraction using 50µl anionic AG1-X8 (200-400 mesh) columns. Samples were loaded and rinsed in 1.5M HBr to elute most of the major and trace elements based on their partition coefficients in hybromic acid[2]. The Pb fraction was collected in 0.5M HNO_3, and purified by a second pass through this column. We note that we have previously tested various acid-leaching protocols on different fractions of an Allende type-B CAI and determined that aggressive acid-leaching, similar to the later steps of the acid-leaching protocol described above, does not produce any measurable Pb isotope fractionation[3].

The total procedural blank for the Pb isotope analyses was decreased during the course of this study from 4.5 pg for the first chemical procedures session in October 2008 (bulk #1) to ~0.7 pg for the second session in December 2008 (mineral separates #2, and #3, and bulk #4) and the measured Pb isotopic composition of each sample was corrected using a 30% uncertainty on the blank contribution for each sample. Details of the blank correction and error correlation calculations are given in Bouvier et al.[5]

Sample preparation and chemical procedures for Al-Mg analyses:

For the Al-Mg analyses, portions from the three interior fractions prepared for the Pb-Pb work (#1, #2 and #3, as described earlier) were taken prior to any chemical processing of these fractions. Also, three additional density separates were prepared from another portion of fraction #3 using bromoform (Geoliquids®; d=2.85) and from an additional interior 30-63 µm size fraction of the 2364-B1 CAI that was subjected to density separation using both methylene iodide and bromoform, respectively. Finally, three additional interior fractions (one composed of

light-colored grains and two mixed fractions with light and dark grains) were hand-picked. Therefore, a total of nine fractions (ranging from ~0.2 to ~3 mg) were dissolved in concentrated HF:HNO_3 (5:1) at 130°C in PFA beakers. These samples were converted to nitrate form in concentrated HNO_3, and then dried down. Samples were then dissolved in 1M HNO_3, and a 5-10% aliquot was reserved for measurements of Al/Mg and Th/U ratios. The equivalent of 1 to 10μg of Mg was then loaded on a cation exchange column packed with pre-cleaned AG50W-X8 (200-400 mesh) resin. Magnesium was eluted from this column (>99% recovery) in 1M HNO_3 and was purified by 3 passes through this column. Details of our chemical procedures for Mg separation are given in Spivak-Birndorf et al.[4].

3) Mass spectrometry

The Pb and Mg isotopic analyses were performed on the ThermoFinnigan Neptune multicollector inductively coupled plasma mass spectrometer (MC-ICPMS) in the Isotope Cosmochemistry and Geochronology Laboratory (ICGL) at ASU equipped with 9 Faraday collectors and 3 ion counters. The Pb-Pb and Al-Mg isotopic data are presented in Table 1, and Tables S1 and S2.The purified Pb samples were dissolved in 3% HNO_3, and were doped with Tl (to allow internal correction of the instrumental mass bias) in a 2:1 proportion; typical concentrations of the sample solutions were 2ppb Pb – 1ppb Tl. We note that measurements have been made of the NBS 981 Pb standard in our laboratory, comparing the Tl-doping and Pb double spike methods of mass bias correction; the measured mass bias corrected $^{207}Pb/^{206}Pb$ ratios in both cases agree with each other, as well as with the $^{207}Pb/^{206}Pb$ ratio measured by thermal ionization mass spectrometry using the double spike method[11] (Fig. S3).

DOI: 10.1038/NGEO941

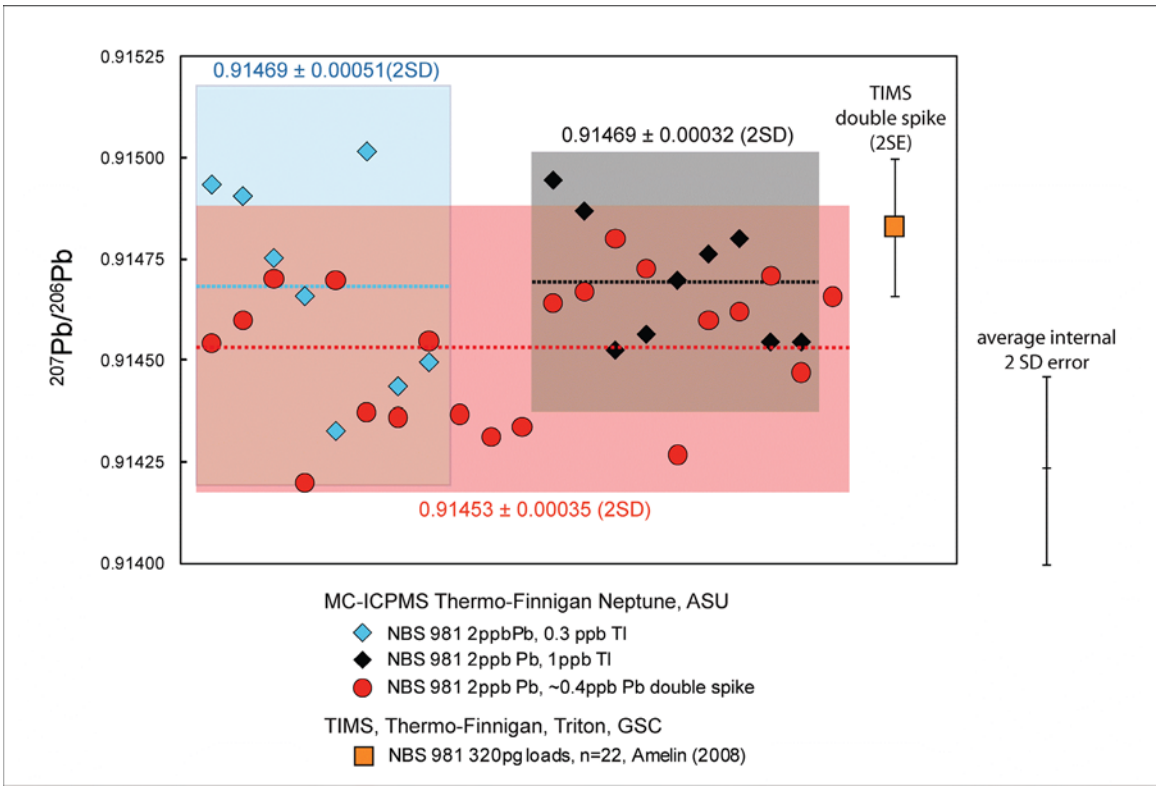

Fig S3: Comparison of $^{207}Pb/^{206}Pb$ ratios measured in 2 ppb total Pb NBS 981 standard solutions during 1-day sessions using the ThermoFinnigan Neptune MC-ICPMS at ASU mass bias corrected using the ^{203}Tl-^{205}Tl Tl-doping method (with 0.3 ppb and 1 ppb total Tl; blue and black diamonds, respectively) or the ^{205}Pb-^{202}Pb double spike method (~0.3 ppb total Pb; red circles) (the averages and 2SD errors for each of these three sets of MC-ICPMS data are shown as the colored dashed lines and colored shaded boxes; the average 2SD internal error for each individual measurement is shown in black). Also shown for comparison here (yellow square) is the average $^{207}Pb/^{206}Pb$ ratio for NBS 981 measured using a thermal ionization mass spectrometer (22 runs, measured over 8 months), with each run comprised of ~320pg Pb NBS 981 and mass bias corrected using the Pb double spike.[11] As can be seen from this figure, the $^{207}Pb/^{206}Pb$ ratios measured by MC-ICPMS (using either Tl-doping or Pb double spike for mass

bias correction) agree well with the value measured by TIMS (using the Pb double spike method for mass bias correction).

Simultaneous measurement of Pb and Tl isotopes was conducted using the axial secondary electron multiplier for ^{204}Pb, and Faraday cups (with 10^{11} ohm amplifiers) for ^{200}Hg, ^{202}Hf, ^{203}Tl, ^{205}Tl, ^{206}Pb and ^{207}Pb. Sample and standard solutions were introduced into the mass spectrometer using the Apex desolvating system with a 50µl/min flow rate nebulizer, which gave a total Pb signal of ~250V/ppm; the background on ^{204}Pb measured on the secondary electron multiplier was typically ~70-100 counts/s. The instrumental blank was measured on a 3% HNO_3 solution before each sample measurement. Each sample was bracketed by a Pb standard (NBS 981 or NBS 983) to correct for instrumental mass bias and to monitor the external reproducibilities on the Pb isotope ratios. Due to the highly radiogenic compositions of our samples (^{206}Pb/^{204}Pb ratios > 1000 for all leachates following L_4), we used the external reproducibilities of NBS 981 for ^{207}Pb/^{206}Pb ratios (±0.0203%, 2SE; n=13), and of NBS 983 for ^{206}Pb/^{204}Pb ratios (±1.33%, 2SE; n=6), and used a correlation coefficient of 0.16 between these two ratios[5] for isochron age calculations using Isoplot version 3.64 by Ludwig[6].

The Mg isotope ratio measurements were made in medium resolution on the ThermoFinnigan Neptune MC-ICPMS. The analytical protocol for measuring Mg isotopes was generally similar to that described by Spivak-Birndorf et al.[4], except as noted here. Purified Mg samples were dissolved in 3% HNO_3 and typical concentrations of sample solutions were ~150-250 ppb. Sample and standard solutions were introduced into the mass spectrometer using the Apex desolvating system with a 100µl/min flow rate nebulizer, which gave a total Mg signal of

DOI: 10.1038/NGEO941

~25V/ppm. The instrumental blank was measured on a 3% HNO_3 solution before each sample measurement. Each sample was bracketed by a Mg standard (DSM3) of similar concentration (within 10%) to correct for instrumental mass bias. The radiogenic ^{26}Mg excess in per mil ($\delta^{26}Mg^*$) in a sample is calculated by normalizing the measured $^{26}Mg/^{24}Mg$ ratios in the sample and bracketing standards to a $^{25}Mg/^{24}Mg$ ratio of 0.12663[7] using the exponential law and a β value of 0.514 (as suggested by Davis et al.[8], for highly fractionated samples such as CAIs), and then comparing the normalized $^{26}Mg/^{24}Mg$ ratio in the sample to the mean of the normalized ratios in the bracketing standards (Table S2). The $^{27}Al/^{24}Mg$ ratios were measured on chemically unprocessed aliquots of sample solutions that had been reserved for this purpose using Faraday cups in static mode (^{24}Mg on Low-3, ^{25}Mg on axial, ^{26}Mg on High-1, and ^{27}Al on High-4) in medium resolution by ThermoFinnigan Neptune MC-ICPMS using a protocol similar to that described by Spivak-Birndorf et al.[4] Accuracy and reproducibility of the measured $^{27}Al/^{24}Mg$ ratios were verified through analyses of rock and mineral standards of known compositions (San Carlos olivine, Allende whole-rock, BCR-2 basalt, AGV-1 andesite, and JR-1 rhyolite) during each analytical session.

Measurements of Th/U ratios were made on the remaining portions of the same sample aliquots on which Al/Mg ratios were measured. Additionally, Th/U ratios were also measured on two bulk fractions (interior and rim) of the 2364-B1 CAI that were hand-picked specifically for this purpose and rinsed only in Milli-Q water prior to dissolution. Depending on the expected amount of U in the samples, $^{232}Th/^{238}U$ ratios were measured either in static mode on Faraday cups or in dynamic mode on the axial secondary electron multiplier, by first analyzing a set of 6 gravimetrically prepared elemental standard solutions with Th/U ratios ranging from 0.10 to 10 to generate a calibration curve. The samples were then analyzed, followed by a second set of

analyses of the gravimetric standard solutions to verify the calibration curve. The true Th/U ratios of the samples (Table S2) were determined from the measured Th/U ratios using the calibration curve based on analyses of the set of gravimetric standards. Based on the accuracy and reproducibility of repeated measurements of the standard solutions, and of the BCR-2 basalt standard (Th/U=3.26 ± 0.16, 2SD), we estimate an uncertainty of ±10% (2SD) on the Th/U ratios determined for these samples.

Supplementary Information: figures

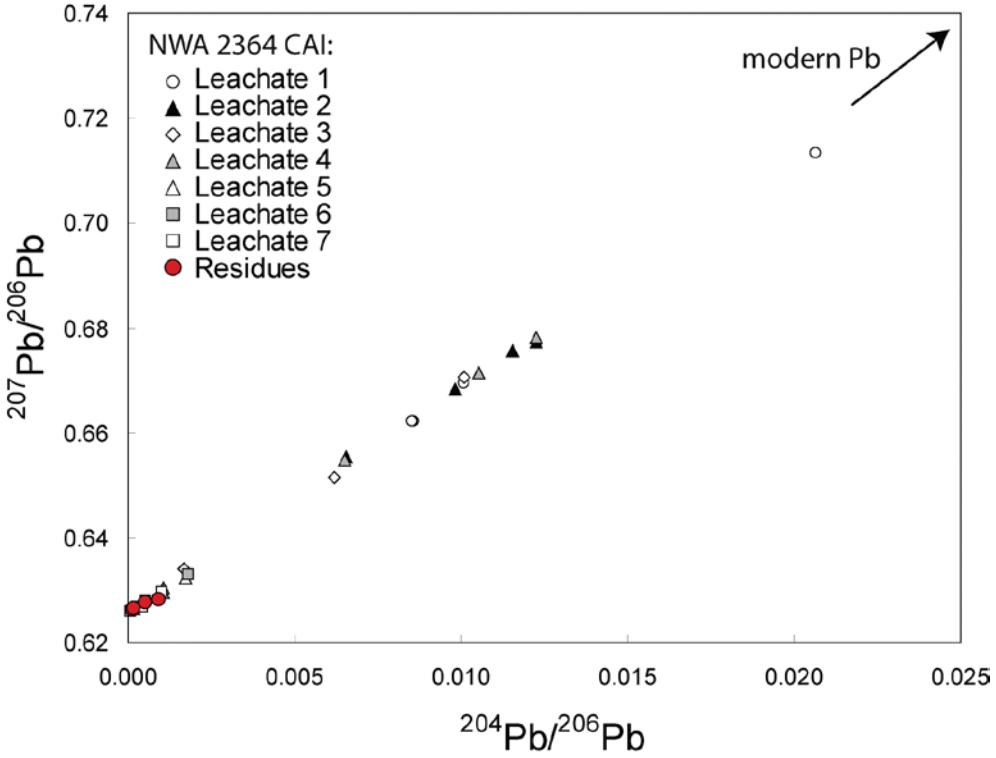

Fig. S4. A plot of $^{207}Pb/^{206}Pb$ versus $^{204}Pb/^{206}Pb$ ratios in the four residues and 7 respective leachates of the four (bulk and mineral separate) fractions of the type-B CAI (2364-B1) from NWA 2364 showing the progressive removal of common Pb through the seven-step leaching protocol; later leachates are increasing more radiogenic. Data for the residues from the three

DOI: 10.1038/NGEO941

interior fractions (#1, #2 and #3) and the last leachates (L7) of each of these fractions are given in Table 1; the data for all other leachates from these fractions and for the residue and leachates of the rim fraction (#4) are shown in Table S1. Errors are smaller than the symbols.

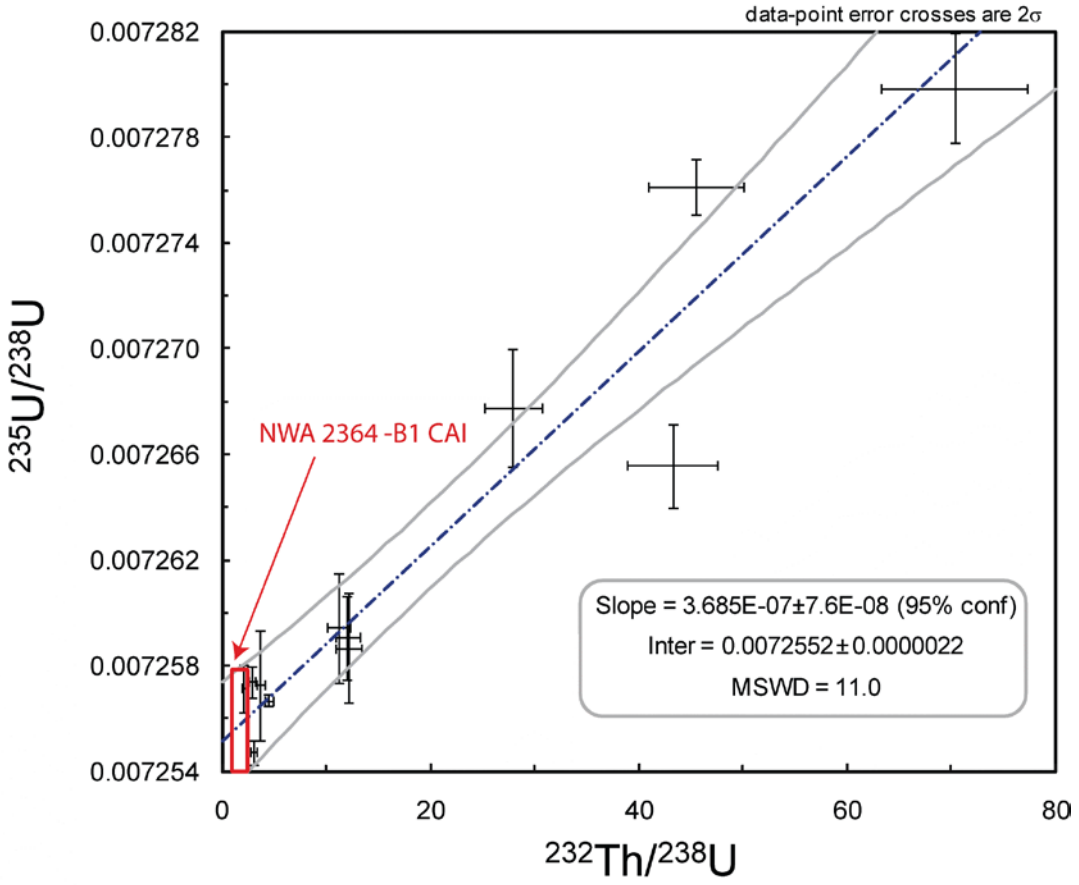

Fig. S5: Figure adapted from Brennecka et al.[9], showing the measured $^{232}Th/^{238}U$ ratio plotted vs. U isotopic composition of Allende CAIs[9], normalized to $^{238}U/^{235}U_{SRM\ 950}$ = 138.84 (ref. 10). The red rectangle illustrates the range of $^{235}U/^{238}U$ ratios estimated for CAI 2364-B1 (i.e., 137.81 to 137.82) based on the Th/U (1.1 to 2.8) measured by us in this CAI.

Supplementary Information: data tables

Table S1: Pb-Pb isotope data for leachates L_1-L_6 from each the three interior fractions (#1, #2, and #3), as well as leachates L_1-L_7 and residue of the rim fraction (#4) from the 2364-B1 CAI. Pb-Pb CDT model ages are calculated using $^{238}U/^{235}U$=137.84 (ref. 10).

Samples	Mass (g)	Total Pb (ng)	$^{206}Pb/^{204}Pb$ mass bias corrected	$^{206}Pb/^{204}Pb$ blank corrected	$^{206}Pb/^{204}Pb$ correlated error (%)	$^{207}Pb/^{206}Pb$ blank corrected	$^{207}Pb/^{206}Pb$ correlated error (%)	Sample/blank ^{206}Pb	Sample/blank ^{204}Pb	CDT model age (Ma)	+/- Ma
#1: Bulk fraction, interior	0.142										
Leachate 1		8.7	98.863	98.997	0.07	0.669375	0.026	3031	447	4564.59	0.43
Leachate 2		8.2	152.74	153.10	0.09	0.655491	0.027	2980	275	4569.84	0.42
Leachate 3		4.4	591.20	601.20	0.55	0.633920	0.024	1781	39	4570.24	0.35
Leachate 4		2.7	916.91	957.43	1.44	0.630509	0.022	1100	15	4568.69	0.33
Leachate 5		17.3	2696.9	5255.5	1.19	0.626339	0.022	7290	18	4567.89	0.32
Leachate 6		6.3	5067.0	5937.1	3.59	0.626479	0.025	2693	6	4567.98	0.35
#2: Pyroxene (fassaite)-rich fraction, 63-100μm	0.033										
Leachate 1		1.6	48.370	48.404	0.08	0.713228	0.026	2468	1023	4554.46	0.54
Leachate 2		0.3	101.09	101.77	0.43	0.668314	0.072	635	95	4565.04	1.20
Leachate 3		low	-					-	-		
Leachate 4		0.2	93.880	94.976	0.56	0.671543	0.060	337	52	4565.24	1.10
Leachate 5		5.8	2398.8	2418.2	0.44	0.627025	0.012	15324	83	4567.16	0.17
Leachate 6		0.7	3502.8	3670.3	1.90	0.626844	0.014	4122	15	4568.21	0.29
#3: Melilite-anorthite-rich fraction, 63-100μm	0.048										
Leachate 1		3.2	116.61	116.73	0.08	0.662199	0.017	5108	909	4563.85	0.28
Leachate 2		1.2	86.484	86.596	0.12	0.675672	0.020	2680	468	4564.09	0.35
Leachate 3		0.4	98.842	99.335	0.27	0.670564	0.028	831	122	4568.02	0.51
Leachate 4		0.4	81.312	81.637	0.21	0.678080	0.025	809	145	4562.14	0.48
Leachate 5		6.2	580.04	581.09	0.14	0.632300	0.010	16119	359	4565.81	0.14
Leachate 6		1.4	552.66	556.88	0.31	0.632859	0.013	3806	90	4566.33	0.24

DOI: 10.1038/NGEO941

#4: Bulk fraction , rim	0.077									
Leachate 1	5.6	116.9	117.00	0.07	0.662028	0.017	8838	1568	4563.64	0.28
Leachate 2	2.3	81.4	81.456	0.05	0.677254	0.019	4930	913	4559.65	0.32
Leachate 3	0.1	155.7	161.35	1.79	0.651510	0.103	202	19	4563.76	1.90
Leachate 4	0.7	153.5	154.22	0.23	0.654798	0.016	1490	142	4568.65	0.27
Leachate 5	8.0	956.2	958.40	0.15	0.629502	0.013	20931	283	4566.37	0.18
Leachate 6	1.7	1856.7	1897.5	0.84	0.627738	0.011	4614	32	4567.64	0.29
Leachate 7	1.2	2224.2	2325.3	1.60	0.626860	0.015	2737	16	4566.59	0.29
Residue	0.7	1039.9	1068.5	1.01	0.628098	0.018	2060	25	4564.21	0.30

Table S2: Al-Mg isotopic data and Th/U ratios in various fractions from the 2364-B1 CAI.

Samples	Mass (mg)	Th/U +/- 10%	$^{27}Al/^{24}Mg$ +/- 2%	n repeats	$\delta^{25}Mg$ per mil	2SE	$\delta^{26}Mg$ per mil	2SE	$\delta^{26}Mg^*$ per mil	2SE
#1: Bulk fraction, interior	2.9	-	2.51	4	4.175	0.018	9.091	0.034	0.959	0.016
#2: Pyroxene-rich fraction, 63-100μm, d>3.3	-	2.4	2.30	4	4.297	0.037	9.205	0.049	0.821	0.035
#3: Melilite-rich fraction, 63-100μm, d<3.3	-	1.8	3.37	4	4.442	0.057	9.914	0.094	1.242	0.049
Interior, 63-100μm, d<2.9	-	2.5	3.63	4	4.365	0.048	9.871	0.060	1.350	0.036
Interior, 30-63μm, 2.9<d<3.3	1.1	2.8	3.33	8	4.326	0.032	9.689	0.053	1.243	0.028
Interior, 30-63μm, d<2.9	0.7	2.3	3.75	8	4.331	0.027	9.843	0.053	1.387	0.018
Hand-picked (light colored) fraction #1	0.2	2.6	4.22	4	4.398	0.006	10.107	0.019	1.518	0.026
Hand-picked (light and dark) fraction #2	1.6	1.1	2.33	4	4.147	0.025	8.952	0.024	0.860	0.030
Hand-picked (light and dark) fraction #3	1.0	2.0	2.32	4	4.263	0.013	9.180	0.015	0.863	0.031

Table S3: CAI model ages calculated using the extinct Al-Mg, Mn-Cr, and Hf-W chronometers, based on isotope systematics measured in the D'Orbigny angrite anchor.

	Initial Ratios	D'Orbigny	ΔT (CAI - D'Orbigny)	CAI Model Age
Pb-Pb age		4564.12 ± 0.12 (ref. 11)		
		4563.36 ± 0.34 (ref. 11, corrected for U isotope composition[10,12])		
$^{26}Al/^{27}Al$	5.2 (± 0.2) $\times 10^{-5}$ (refs. 13, 14)	5.06 (± 0.92) $\times 10^{-7}$ (ref. 4)	4.78 ± 0.19 Ma	4568.2 ± 0.4 Ma
$^{53}Mn/^{55}Mn$	9.1 (± 1.7) $\times 10^{-6}$ (ref. 15)	3.24 (± 0.04) $\times 10^{-6}$ (ref. 16)	5.51 ± 1.00 Ma	4568.9 ± 1.1 Ma
$^{182}Hf/^{180}Hf$	9.72 (± 0.44) $\times 10^{-5}$ (ref. 17)	7.20 (± 0.21) $\times 10^{-5}$ (ref. 18)	3.85 ± 0.69 Ma	4567.2 ± 0.8 Ma

Additional references:

1 Russell, S. S. *et al.* The Meteoritical Bulletin, No. 89, 2005 September. *Meteorit. Planet. Sci.* **40**, A201–A263 (2005).

2 Marsh, S. F., Alarid, J. E., Hammond, C. F., McLeod, M. J. & Rein, J. E. Anion exchange of 58 elements in Hydrobromic acid and in Hydriodic acid. *Los Alamos Sci. Lab. Univ. Calif. Rept.* **7084**, 16 (1978).

3 Bouvier, A., Wadhwa, M. & Janney, P. E. ^{26}Al-^{26}Mg and ^{207}Pb-^{206}Pb systematics in an Allende inclusion. *Meteorit. Planet. Sci.* **41**, abstr. #5299 (2008).

4 Spivak-Birndorf, L., Wadhwa, M. & Janney, P. E. ^{26}Al–^{26}Mg systematics in D'Orbigny and Sahara 99555 angrites: Implications for high-resolution chronology using extinct chronometers *Geochim. Cosmochim. Acta* **73**, 5202–5211 (2009).

5 Albarède, F. *et al.* Precise and accurate isotopic measurements using multiple-collector ICP-MS. *Geochim. Cosmochim. Acta* **68**, 2725-2744 (2004).

6 Isoplot/Ex version 3.64. A Geochronological Toolkit for Microsoft Excel. (Berkeley Geochronology Center, March 17, 2008).

7 Catanzaro, E. J., Murphy, T. J., Garner, E. L. & Shields, W. R. Absolute isotopic abundance ratios and atomic weight of magnesium. *J. Res. Nat. Bur. Stand.* **70a**, 453-458 (1966).

8 Davis, A. M. *et al.* Isotopic mass fractionation laws and the initial solar system ^{26}Al/^{27}Al ratio. *Lunar Planet. Sc. Conf. XXXVI*, A2334 (2005).

9 Brennecka, G. *et al.* ^{238}U/^{235}U Variations in Meteorites: Extant ^{247}Cm and Implications for Pb-Pb dating. *Science* **327**, 449-451, doi:10.1126/science.1180871 (2010).

10 Richter, S. *et al.* New average values for the n(^{238}U)/n(^{235}U) isotope ratios of natural uranium standards. *International Journal of Mass Spectrometry* **In Press** (2010).

11 Amelin, Y. U-Pb ages of angrites. *Geochim. Cosmochim. Acta* **72**, 221-232 (2008).

12 Brennecka, G. *et al.* Toward reconciling early Solar System chronometers: the ^{238}U/^{235}U ratios of chondrites and D'Orbigny pyroxenes. *Lunar Planet. Sc. Conf. XVI*, A#2117 (2010).

13 Jacobsen, B. *et al.* ^{26}Al–^{26}Mg and ^{207}Pb–^{206}Pb systematics of Allende CAIs: Canonical solar initial ^{26}Al/^{27}Al ratio reinstated. *Earth Planet. Sci. Lett.* **272**, 353-364 (2008).

14 MacPherson, G. J. *et al.* Early Solar Nebula Condensates with Canonical, Not Supracanonical, Initial ^{26}Al/^{27}Al Ratios. *The Astrophysical Journal Letters* **711**, L117 (2010).

15 Nyquist, L. E., Kleine, T., Shih, C. Y. & Reese, Y. D. The distribution of short-lived radioisotopes in the early solar system and the chronology of asteroid accretion, differentiation, and secondary mineralization. *Geochim. Cosmichim. Acta* **73**, 5115-5136 (2009).

16 Glavin, D., Kubny, P. A., Jagoutz, E. & Lugmair, G. W. Mn–Cr isotope systematics of the D'Orbigny angrite. *Meteorit. Planet. Sci.* **39**, 693-700 (2004).

17 Burkhardt, C. *et al.* Hf-W mineral isochron for Ca,Al-rich inclusions: Age of the solar system and the timing of core formation in planetesimals. *Geochim. Cosmichim. Acta* **72**, 6177-6197 (2008).

18 Markowski, A. *et al.* Hafnium-tungsten chronometry of angrites and the earliest evolution of planetary objects. *Earth Planet. Sci. Lett.* **262**, 214-229 (2007).